

Regeneration of Hexavalent Chromium from a Simulated Rinse Etching Solution Using an Electrochemical Reactor With Two Compartments Separated by a Ceramic Membrane

M. García-Gabaldón*, V. Pérez-Herranz, Henry Reyes

IEC Group. Departamento de Ingeniería Química y Nuclear. Universidad Politécnica de Valencia. P.O. Box 22012, E-46071 Valencia. Spain.

*E-mail: mongarga@iqn.upv.es

Received: 9 March 2011 / Accepted: 28 April 2011 / Published: 1 May 2011

The performance of a batch electrochemical reactor with two compartments separated by a ceramic diaphragm for the regeneration of Cr(VI) from a simulated rinse etching solution has been studied under constant cell voltage mode and in galvanostatic operation. The effect of the applied current (I) and cell voltage (U) on the Figures of Merit (fractional conversion, current efficiency, space-time yield and specific energy consumption) for the Cr(III) to Cr(VI) electrochemical oxidation is analyzed. As both I and U parameters increase, the current efficiency (ϕ) for the electrochemical oxidation of Cr(III) is decreased due to the oxygen evolution side reaction, which causes an increment in the specific energy consumption (E_s). On the other hand, an increment of the values of I and U leads to greater values of both Cr(III) fractional conversion (X) and space-time yield (η) due to the oxygen turbulence-promoting action. Comparing the results obtained under both operation modes, in galvanostatic operation higher values of X, η and ϕ coupled with lower values of E_s are obtained. Hence, working in galvanostatic operation at a relatively low applied current (1.5A) is the optimum option since the energy consumed is quite low, the current efficiency is relatively high and the amount of Cr(VI) recovered is close to 70%.

Keywords: Ceramic diaphragms, electrochemical oxidation, hexavalent chromium regeneration, rinse etching solution, trivalent chromium.

1. INTRODUCTION

Metallization of plastics is normally undertaken for either decorative or functional purposes. Through metallization, the specific properties of plastics, such as light weight, design flexibility and low cost of manufacturing, are enhanced by the addition of properties usually associated with metals. These include reflectivity, abrasion resistance, electrical conductivity and a variety of decorative

effects [1]. Metal-plated plastics find use in the automotive industry, hardware, plumbing fixtures, knobs, RFI-EMI-shielding and electronic applications. The bond strength between the metal plate and the plastic is of great importance in the final product [2].

The electroless plating of polymers consists of the following steps: brushing, etching, neutralization, activation, acceleration and electroless plating. The etching stage is responsible for fully developing suitable conditions for good metal-plastic adhesion. This step consists of the immersion of the plastic sheets in an oxidant solution. The usual oxidant solutions are composed of chromic acid in aqueous sulphuric acid. During the etching stage, the hexavalent chromium (in the form of $\text{Cr}_2\text{O}_7^{2-}$) is reduced to trivalent chromium. As Cr(III) builds up in the chromic acid bath during use, a portion of the baths must be discharged even though it still contains large amounts of chromic acid [3]. On the hand, although in the rinse etching baths the concentration of hexavalent chromium is considerably lower, the big volumes generated represent an important problem. Since disposal of chromic acid is difficult, it is increasingly attractive to regenerate the waste chromium liquors [4].

Compounds of Cr(VI) have been related as very toxic mainly due to their confirmed carcinogen action. In face of this toxic effect, chromium concentrations in industrial effluents are strictly controlled before being discharged into sewages or rivers [5, 6], which is a major environmental issue, affecting every industrialized country in the world [7, 8]. Owing to the solubility and high toxicity of the Cr(VI) oxo-anions, the effluents are normally submitted to a chemical reduction that converts Cr(VI) oxo-anions to their inert Cr(III) cations [9]. Other processes based on the direct elimination of Cr(VI) by fixing it on appropriate anion-exchange resins are used on an industrial scale [10-13]. Liquid-liquid extraction and liquid membrane technique have also been explored and found to be able to concentrate Cr(VI) [14, 15]. However, all these techniques are either very less selective or very slow and involve various chemicals and further waste generation.

Among the possible alternatives to the treatment of industrial spent chromic acids, electro-membrane processes offer many advantages. Because of their modularity and profitability at small scale, electro-membrane separation techniques are well suited to the treatment of the pollution at its source [16-21]. Some reports are available for the treatment of Cr(VI) acid solutions by electrodialysis [18, 22, 23], but frequent anion-exchange membrane replacement was required since the membrane worked under severe conditions. In this sense, the porous ceramic material is a relatively inexpensive diaphragm, compared to ion-exchange resins, electrodialysis membranes and semi-permeable polymer diaphragms [24]. On the other hand, inorganic diaphragms have a higher mechanical strength and chemical resistance to attack by oxidizing acids like chromic acid [25]. Mandich et al. [26] and Gudatti et al. [27] reported the use of a ceramic diaphragm for the removal of impurities in spent chromium plating baths using a porous pot technique (PPT).

In this paper we are reporting the regeneration of hexavalent chromium using an electrochemical reactor with two compartments separated by a ceramic diaphragm. Previous experiments with ceramic separators of different porosity and pore size distribution [28, 29] led us to select the ceramic membrane used in the present work as the optimum option from the point of view of the maximum Cr(VI) recovered. The rinse etching bath would be introduced in the anodic compartment of the electrochemical reactor whereas the cathodic compartment is filled up with sulphuric acid. The trivalent chromium present in the rinse etching bath would be oxidized to

hexavalent chromium in the anodic compartment whilst the production of hydrogen would be the main reaction taking place in the cathodic compartment. The use of the ceramic diaphragm is justified in order to minimise the presence of Cr(III) and Cr(VI) in the cathodic compartment, where could be reduced decreasing the current efficiency of the process. The recovery of the hexavalent chromium in the anodic compartment of the electrochemical reactor would simultaneously lower the cost of reagents associated with extending the life of the etching bath and the costs associated with disposal of the contaminated bath.

Two previous papers [30, 31] evaluated the performance of the same electrochemical reactor for the treatment of the activating solutions coming from the electroless plating of polymers under potentiostatic and galvanostatic operation. In this sense, the present paper is the last of a series of three papers which evaluate the treatment of the main effluents generated during the pre-treatment phases of the electroless plating of polymers process by using the same electrochemical reactor in the presence of a ceramic membrane. This work evaluates the effect of the applied current and cell voltage on the "Figures of Merit" of the two-compartment electrochemical reactor in the presence of a simulated rinse etching solution.

2. EXPERIMENTAL SECTION

The experimental setup used in this work was adequately described in previous papers [30, 31]. The electrochemical reactor consisted of two Pyrex glass chambers attached by means of four screws on their sides with a ceramic diaphragm placed between them. The electrodes were totally immersed in the solution. The cathode was made of two cylindrical graphite bars and the anode was a lead alloy. Before use, the lead anode was passivated by passing a positive current (mA) in sulphuric acid solution for 2-4h at a constant electrode potential of 0.4V [32]. If a lead anode is used, almost quantitative production of dichromate results [33] in addition to oxygen evolution. This reaction mechanism involves the oxidation of lead to PbO_2 , which is a catalyst for Cr(III) oxidation. This catalysis is advantageous in reducing Cr(III) concentration [34, 35]. Although this process increases resistivity because lead oxide is poorly conductive, the capital cost of a lead anode is much smaller than platinum and many other potential anodes [32].

Both electrodes were symmetrically separated from the ceramic diaphragm. Experiments were performed at different constant applied currents (1.5A and 2.5A) and cell voltages (10V and 15V) using a power supply (Grelco VD 310). The cell voltage values were selected so as to obtain considerable values of the Cr(III) to Cr(VI) conversion, and the current values were chosen in order to obtain similar values to those recorded in the constant cell voltage experiments. In a potentiostatic operation, a constant potential on the working electrode with respect to a reference electrode is established, and the electrode potential determines which electron transfer reactions can occur and their absolute rates. The potentiostatic way of operation is easy to put into practice on a laboratory scale by using a standard potentiostat. Nevertheless, its industrial scale extension is more difficult because of the elevated cost of potentiostats of high power. Another shortcoming to the potentiostatic mode at industrial scale is the requirement of reliable reference electrodes. Then, for most industrial

electrochemical processes, constant cell voltage and constant current control are the most useful operating approach from both a practical and theoretical standpoint.

Prior to use, the ceramic diaphragm was submerged in 0.5M H₂SO₄ for 24 hours to remove any metal impurities and then washed with distilled water. The main properties of the ceramic membrane used in this work are presented in Table 1. Analytical grade reagents were supplied by Panreac and were used for the preparation of the synthetic solutions. A solution composed of 0.5M H₂SO₄ was poured into the cathodic compartment of the electrochemical reactor, while the anodic compartment was filled with a model rinse etching solution composed of 0.5M H₂SO₄, 0.1M Cr(VI), as CrO₃, and 0.1M Cr(III), as KCr(SO₄)₂·12H₂O. An equal volume (250 cm³) of anolyte and catholyte was poured in their respective chamber after cell assembly. The operating temperature was 298K. Samples were taken from the anolyte at different time intervals, and the values of current and cell voltage were also recorded during electrolysis using a digital multimeter. Hexavalent chromium concentration was determined by titration with Fe(SO₄)₂(NH₄)₂·6H₂O and the determination of total Cr was performed by atomic absorption spectrometry on a Perking Elmer model AAnalyst 100 atomic absorption spectrometer using a chromium hollow cathode lamp at 428.9 nm wavelength, 0.2nm spectral bandwidth and an operating current of 7mA. The concentration of Cr(III) was calculated by difference between the total chromium and the Cr(VI) values.

Table 1. Properties of the ceramic diaphragm

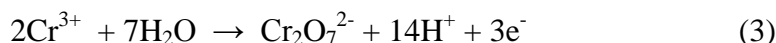
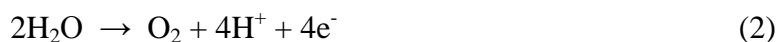
| Property | Ceramic membrane |
|--|---|
| Composition | 50.5% kaolin; 49.5% alumina |
| Manufacture pressure (kg·cm ⁻²) | 250 |
| Porosity (cm ³ of pores/cm ³ of separator) | 0.50 |
| Diameter of pore medium (μm) | 0.37 |
| Thickness (cm) | 0.67 |
| Effective area of membrane (cm ²) | 11.1 |
| Electrical resistance (Ω) ^a | 630 |
| Characteristics | High diffusion and convection resistances |

^a Measured by equilibrating with a 10⁻³M HCl solution at 298 K

3. RESULTS AND DISCUSSION

The variation of current with time for the different cell voltages is presented in Fig. 1. Current initially increases, and then, after attaining a maximum value, it decreases (15V) or remains practically constant (10V) with time. At the beginning of the process, the overvoltage is very high due to the time needed for the activation of the electrode, and consequently, initially the current reached is low. On the lead alloy anodes used in the present work, the first reaction that takes place is the oxidation of the

anode to a chocolate-brown lead dioxide (known as “activation step”). On this surface, there are two reactions that occur during plating. The predominant reaction is the generation of oxygen, and the second one is the oxidation of trivalent chromium to hexavalent chromium ions. The rate of this reaction is largely determined by the mass transport of the trivalent ion to the anode surface. The reactions can be represented in a simplified form as follows [36]:



Once the PbO_2 layer is formed on the anode surface according to reaction (1), current increases and remains almost constant for an applied cell voltage of 10V (Fig. 1), since for this value the Cr(III) oxidation to Cr(VI) is relatively slow. For an applied cell voltage of 15V, Cr(III) oxidation is quite fast, and consequently, its concentration in solution is considerably decreased which causes the appearance of a concentration overvoltage responsible for the current decrease.

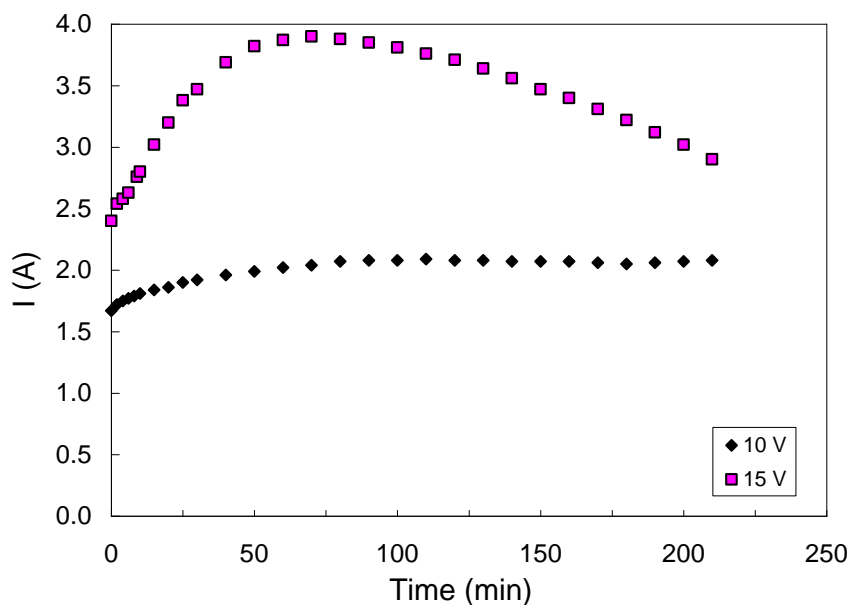


Figure 1. Variation of current with time at different applied cell voltage

In the case of galvanostatic operation (Fig. 2), cell voltage initially presents a high value (between 15V and 20V) which corresponds to the minimum cell voltage necessary to start the oxidation of the lead anode to PbO_2 . As a consequence of the electrode activation and the decrease of the electrode overvoltage for Cr(III) oxidation, cell voltage decreases to reach a constant value of 9V and 11.5V for the respective applied currents of 1.5A and 2.5A.

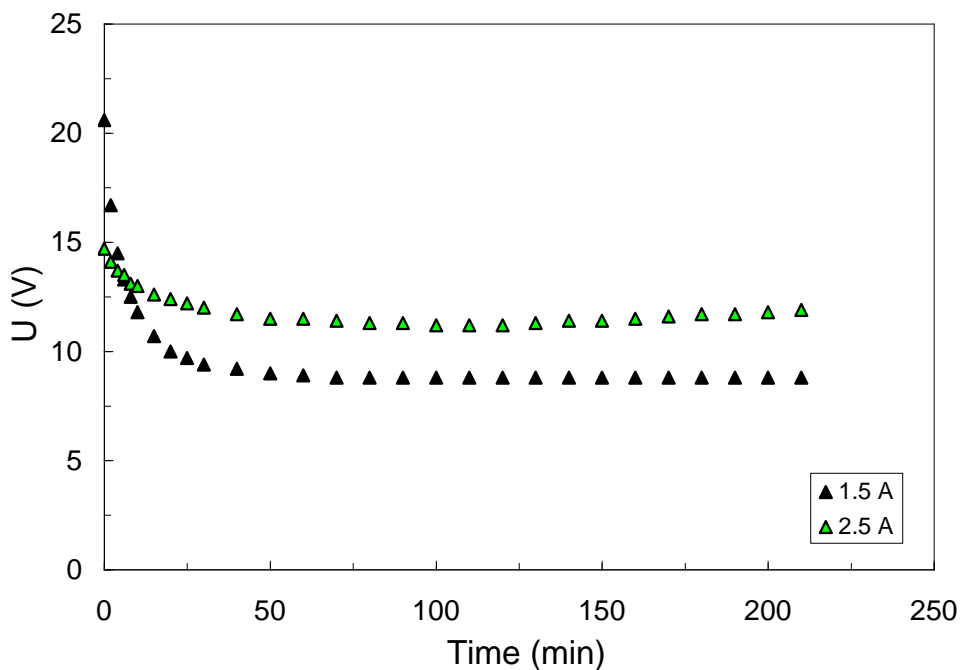


Figure 2. Variation of cell voltage with time at different applied currents

Under both operation modes, constant cell voltage and constant current, when the current is switched on, there is an immediate production of oxygen at the anode and hydrogen at the cathode. Since H⁺ ions are produced by the oxidation reactions at the anode they will pass through the membrane to be reduced at the cathode since protons are very mobile [29]. For this reason, Cr(III) ions remain in the anolyte chamber for the longest time and have greatest chance of being anodically oxidised [37].

For any process, the study of the recovery product, i.e. the conversion (X) and the space-time yield (η), is highly important to predict its commercial viability. On the other hand, current efficiency (φ) and energy consumption (E_s) are significant parameters for assessing the suitability of any electrochemical process for practical application. These parameters are the “Figures of Merit” of the electrochemical reactor, and are defined for the process of Cr(III) to Cr(VI) oxidation as follows:

$$X(t) = \frac{C_0 - C(t)}{C_0} \tag{4}$$

$$\phi(t)(\%) = \frac{nF(C_0 - C(t))V}{\int_0^t I(t)dt} \times 100 \tag{5}$$

$$\eta(t)(g\ l^{-1}h^{-1}) = \frac{M(C_0 - C(t))}{t} \tag{6}$$

$$E_s(t)(kWhkg^{-1}) = \frac{\int_0^t U(t)I(t)dt}{3600VC_0X(t)M} \tag{7}$$

The evolution of the fractional conversion vs. time referred to the Cr(III) oxidation to Cr(VI), under constant cell voltage and in galvanostatic operation is presented in Figures 3 and 4, respectively. X increases with the increase of the cell voltage as for the highest cell voltage (15V) global current is higher, which means that the velocity of the oxidation reaction of Cr(III) is greater (Fig. 3). A dead time of about 20 minutes is clearly observed for both applied cell voltages under study. During this period of time, the hexavalent chromium recovered is practically null due to the low currents passing through the reactor. This is a consequence of the activation of the electrode surface as the lead dioxide must be formed previously to the Cr(III) oxidation according to reaction (1). For time values higher than 20 minutes, the fractional conversion increases with time and tends asymptotically to a final value, this behaviour being characteristic of a stirred batch reactor.

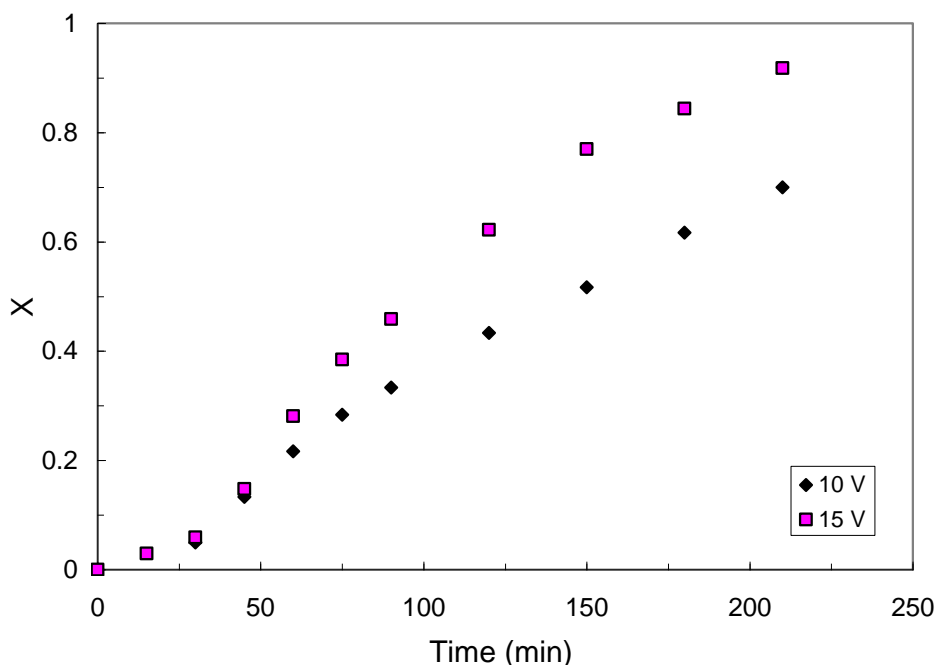


Figure 3. Fractional conversion of Cr(III) versus time for different cell voltages

The effect of the applied current on the fractional conversion of Cr(III) is shown in Fig. 4. It is seen that X increases with increasing both electrolysis time and current, since the latter parameter is proportional to the velocity of the electrochemical reaction that takes place. Under galvanostatic operation, the activation of the electrode is faster than in the case of constant cell voltage, as imposing a current value is equivalent to fix the velocity of the oxidation reactions. This fact is reflected by the absence of the dead time observed previously in Fig. 3.

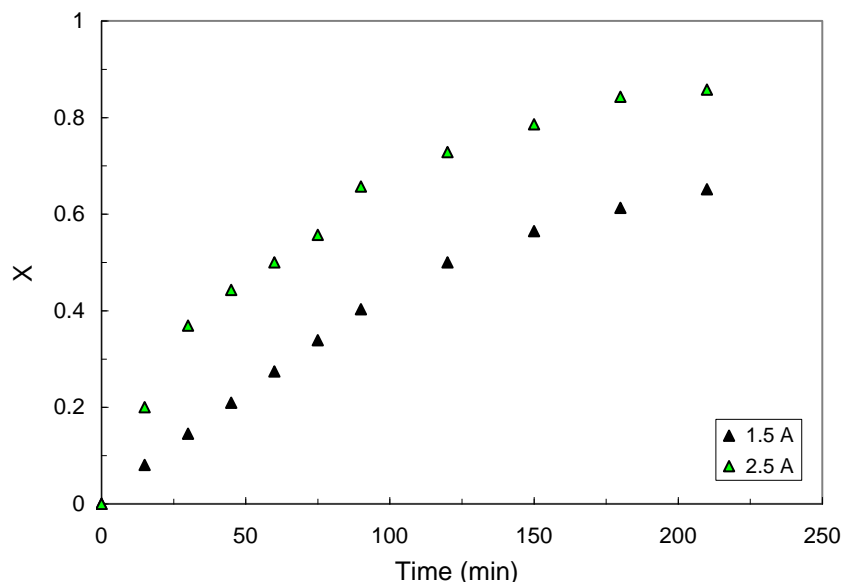


Figure 4. Fractional conversion of Cr(III) versus time for different applied currents

The current efficiency evolution with time for the different cell voltages is plotted in Fig. 5. ϕ decreases with increasing the cell voltage due to the significant extend of oxygen formation in the anode. For both cell voltages under study, current efficiency presents a maximum value. Initially, ϕ is low and is the consequence of the activation period of the anode, this behaviour is similar to that observed previously for global current (Fig. 1). As the Cr(III) is oxidised to Cr(VI), current efficiency becomes greater and once Cr(III) is depleted from solution, ϕ starts to decrease due to the contribution of the secondary reactions, i.e the production of oxygen gas. Regardless of the applied cell voltage, the maximum values of ϕ are quite low (around 20%) and are typical of the electrochemical oxidation and reduction of chromium [27].

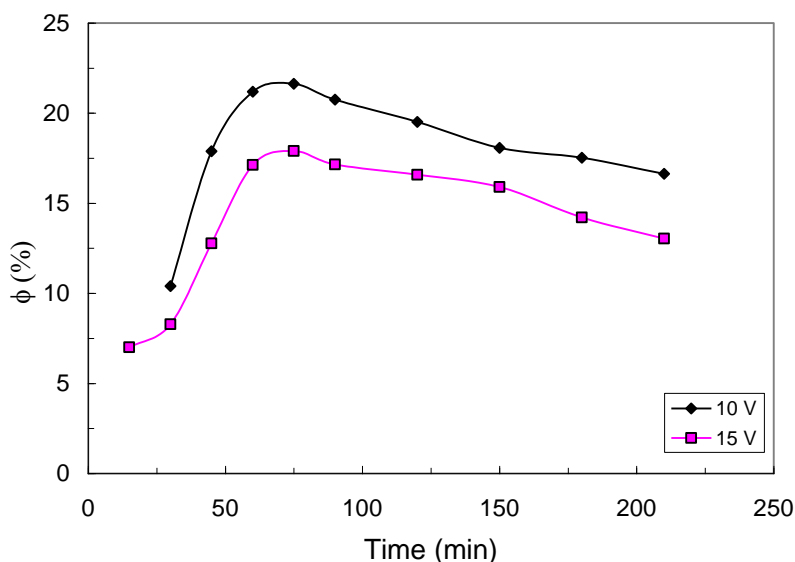


Figure 5. Current efficiency versus time for different cell voltages

The evolution of current efficiency with time for the different applied currents is shown in Fig. 6. For a current value of 1.5A, ϕ reaches a maximum value of 42% when the electrolysis time is close to 30 minutes whereas for the highest current value the maximum ϕ obtained is about 70%. Afterwards, the current efficiency decreases since the amount of Cr(III) in solution is considerably lower and secondary oxidation reactions become important. If the electrolysis time is higher than 100 minutes, ϕ decreases with the increase of the applied current since higher applied currents result in the evolution of oxygen (as seen from the vigorous evolution of gas bubbles from the anode), which reduces the anode efficiency. This is because, at higher applied currents, the oxidation potential of Cr(III) and that of oxygen evolution become closer to each other [38]. When the cell voltage was constant, the initial value of ϕ was lower (Fig. 5) as the activation of the electrode was slower under this operation mode. On the other hand, the final value of current efficiency is higher under galvanostatic operation, and although this value is relatively small, is in the range expected for processes of oxidation/reduction of chromium.

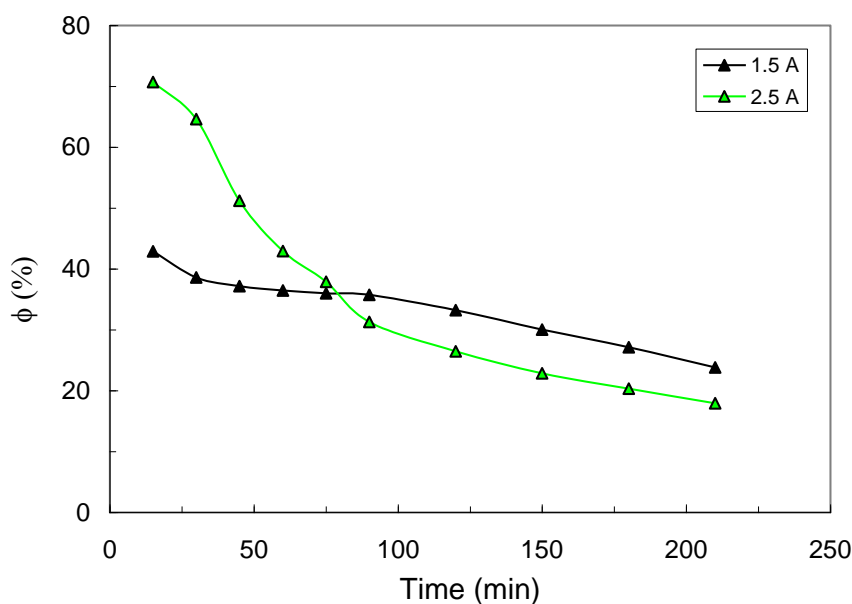


Figure 6. Current efficiency versus time for different applied currents

The space-time yield under constant cell voltage follows the same tendency as that observed for global current as shown in Fig. 7. The initial increase of the space-time yield can be attributed to catalytic layer formed on the anode surface which causes a decrease in the electrode resistance for the Cr(III) oxidation.

Then, it decreases slowly with time due to the removal of Cr(III) from the solution. For a given time value, the space-time yield increases with the applied cell voltage because oxygen evolution likely modifies the electrolyte flows at the vicinity of the anode surface, and an increase in the mass transfer rate actually results from the forced convection [39].

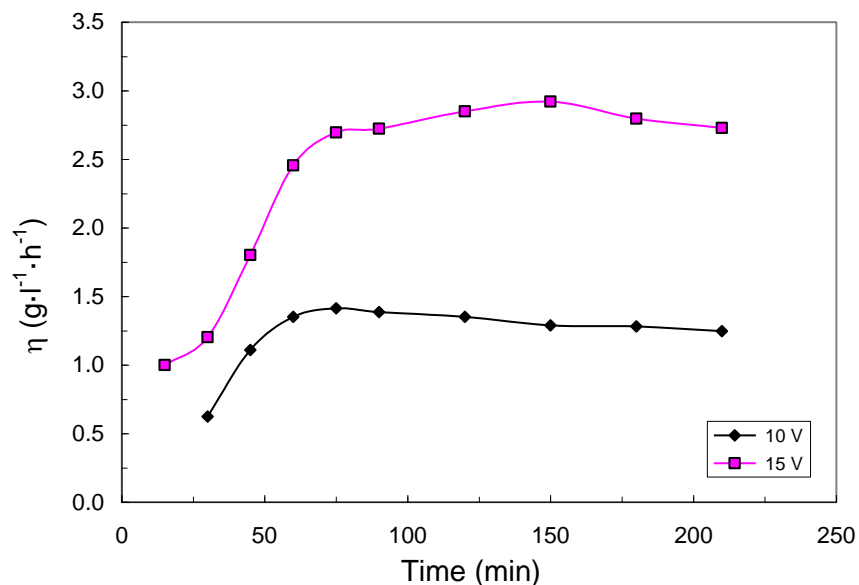


Figure 7. Space-time yield versus time for different cell voltages

As observed in Fig. 8, the space-time yield decreases with time for the different applied currents as the Cr(III) species are removed from solution. This behaviour differs from that observed under constant cell voltage (Fig. 7) since working under galvanostatic operation is equivalent to fix the velocity of the Cr(III) oxidation reaction, and the anode activation is assumed to be quite fast for both applied currents under study. On the other hand, as shown in Fig. 8, the higher the applied current the bigger the amount of Cr(III) oxidised to Cr(VI) due to the turbulence-promoting action of the oxygen bubbles generated in the anode that enhance the mass transfer of Cr(III) towards the electrode surface [30, 40].

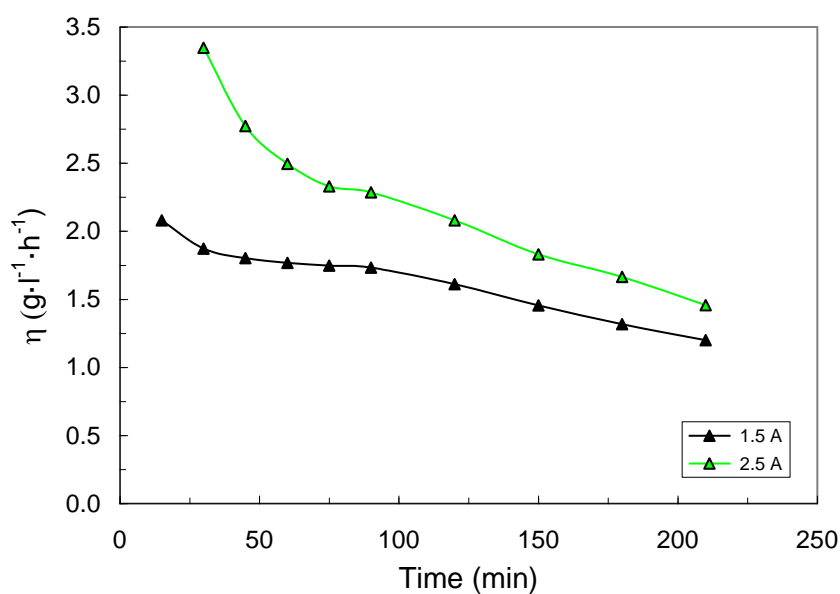


Figure 8. Space-time yield versus time for different applied currents

The effect of the cell voltage on the evolution of the specific energy consumption with time is shown in Fig. 9. E_s is very high at the beginning of the process as a consequence of the time needed for the activation of the anode to be completed, then as Cr(III) is removed from solution, E_s decreases to reach a value which remains practically constant. The last part of the curve obtained at 15V presents a slight increase of E_s which reflects the greater contribution of the oxygen evolution as side cathodic reaction.

In the case of the highest cell voltage value (15V), the energy consumed is higher than that observed for 10V, as although the amount of Cr(III) oxidised to Cr(VI) is greater, global current is always higher as well.

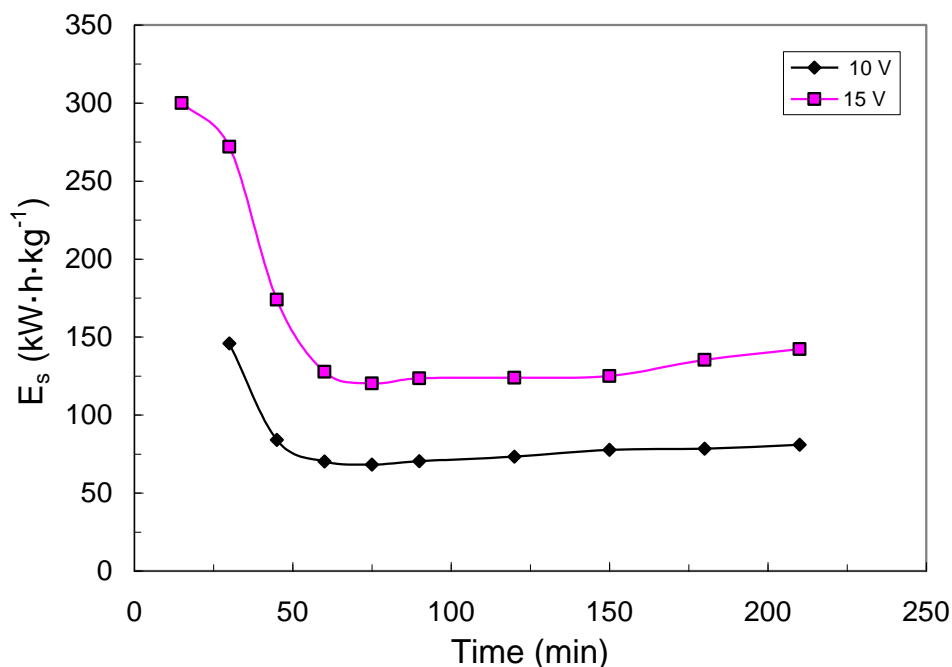


Figure 9. Energy consumption versus time for different cell voltages

The effect of the applied current on the evolution of the specific energy consumption with time is shown in Fig. 10.

The increase of E_s with the applied current can be attributed to the decrease in current efficiency because of the onset of the oxygen evolution. For an applied current of 1.5A, as Cr(III) is depleted from solution, E_s decreases slowly with time up to an electrolysis time close to 100 minutes. Beyond this value, since the Cr(III) concentration is very low, oxygen evolution becomes more important, and consequently, the energy consumed is increased. At 2.5A, the energy consumed increases continuously with time because the applied current is so high that the secondary reactions are present from the beginning of the experiments.

Comparing the behaviour of E_s in both operation modes, it is inferred that this parameter is lower under galvanostatic operation.

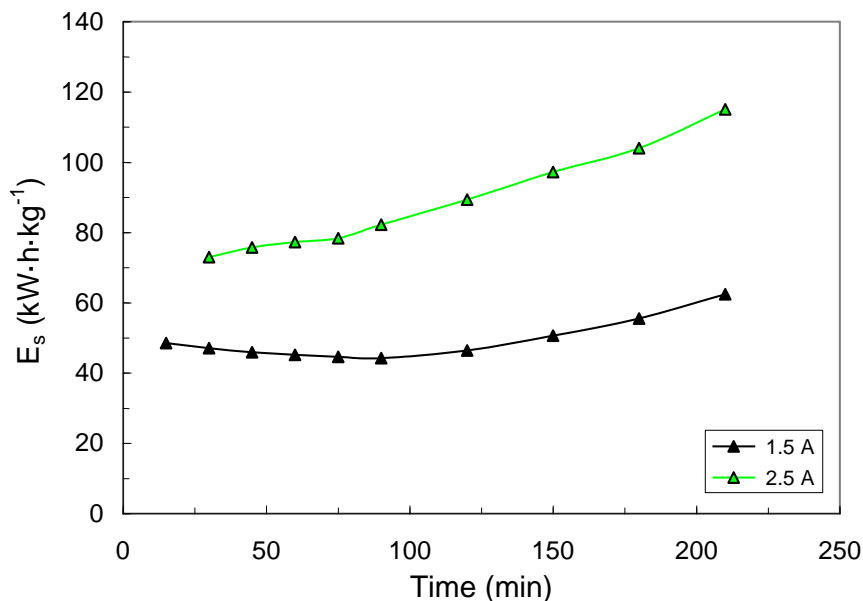


Figure 10. Energy consumption versus time for different applied currents

In order to compare the performance of the electrochemical reactor for the different applied currents and cell voltages, the time (t_{100}) at which a 100% Cr(III) fractional conversion is reached, assuming a current efficiency of 100%, has been determined from the following equation:

$$\int_0^{t_{100}} I \cdot dt = n \cdot F \cdot V \cdot C_0 \tag{8}$$

where t_{100} represents the time when the charge passed in the reactor corresponds to the stoichiometric value. In the particular case of galvanostatic operation, this parameter can be determined from the following equation, since the applied current keeps constant:

$$t_{100} = \frac{n F V C_0}{I} \tag{9}$$

For both operation modes, the values of the four figures of merit corresponding to t_{100} have been evaluated and are reported in Table 2. As a consequence of the increase in the Cr(III) electrochemical oxidation rate with the applied current and cell voltage, t_{100} decreases with the increase in both variables. Under both operations modes and for t_{100} , the fractional conversion and the space-time yield increase with the applied current and cell voltage because of the increase in the oxidation rate of Cr(III). In addition, the increase in X and η is also due to the turbulence-promoting action of the oxygen evolution. On the other hand, the formation of oxygen as a secondary reaction produces a drop in current efficiency with the increase in both current and cell voltage. The energy consumption considerably increases due to the increment in current and cell voltage, and the decrease in current efficiency.

Table 2. Figures of merit for the electrochemical Cr(III) oxidation

| | $t_{100}(\text{min})$ | X | ϕ (%) | $\eta(\text{g l}^{-1} \text{h}^{-1})$ | $E_s(\text{kW h kg}^{-1})$ |
|-------|-----------------------|------|------------|---------------------------------------|----------------------------|
| 10 V | 60.9 | 0.22 | 21.2 | 1.35 | 70.2 |
| 15 V | 59.2 | 0.27 | 16.7 | 2.42 | 130.2 |
| 1.5 A | 47.9 | 0.39 | 36.6 | 1.74 | 45.2 |
| 2.5 A | 45.5 | 0.41 | 34.8 | 2.76 | 78.8 |

Comparing the results obtained under both operation modes for t_{100} , greater values of the fractional conversion, space-time yield and current efficiency coupled with lower values of energy consumed are obtained in galvanostatic operation. Hence, a current value of 1.5A is chosen as best option since the amount of Cr(VI) recovered is close to 70%, the energy consumed is quite low, and consequently, the current efficiency obtained (around 37%) is under the expected values for a chromium oxidation/reduction process.

4. CONCLUSIONS

The disposal of the rinse etching solutions present in the plating of polymers industry is problematic due to the presence of hexavalent chromium, hence, its recycling and regeneration is always preferably from the point of view of economy and environment. In this sense, the present paper evaluates the oxidation of Cr(III) to Cr(VI) in a two-compartment cell. The anolyte and catholyte are separated by a ceramic membrane to prevent the cathodic reduction of Cr(III) and Cr(VI) both present in the rinse etching baths. The major electrochemical reaction on the cathode is the hydrogen evolution whilst the main reactions occurring in the anode are the continuous oxidation of Cr(III) to Cr(VI) and the oxygen evolution once the lead anode has been activated.

Important parameters like fractional conversion, current efficiency, space-time yield and energy consumption have been calculated as a function of experimental variations of cell voltage and global current. Low global current values and cell voltages are the most optimum because an increase in both parameters results in the evolution of oxygen gas which reduces the current efficiency of the process. The increase in global current also increases the energy consumption. On the other hand, high values of current and cell voltage also leads to higher values of the fractional conversion and the space-time yield, which is explained by the turbulence-promoting action of the oxygen evolution.

Comparing the results obtained under both operation modes, higher values of the fractional conversion, space-time yield and current efficiency coupled with lower values of energy consumed are obtained in galvanostatic operation. Hence, working at a relatively low applied current (1.5A) is the optimum option since the amount of Cr(VI) recovered is close to 70%, the energy consumed is

considerably low and the current efficiency is under the expected values for a chromium oxidation/reduction process (around 37%).

ACKNOWLEDGEMENTS

We wish to express our gratitude for the support of this work by the Ministerio de Ciencia e Innovación (convention no. CTQ2008-06750-C02-01/PPQ).

References

1. L.A.C. Teixeira and M.C. Santini, *J. Mater. Process. Tech.*, 170 (2005)
2. S. Hempelmam, *Tratamiento de Superficie*, 87 (1998) 24
3. S. Beszedits, *Chromium removal from industrial wastewaters. Chromium in the Natural and Human Environment*, John Wiley & Sons, New York 1988)
4. D. Pletcher and F.C. Walsh, *Industrial Electrochemistry*, Blackie Academic & Professional, New York (1993)
5. H.G. Seiler, H. Sigel and A. Sigel, *Handbook of toxicity of Inorganic Compounds*, Marcel Dekker, New York (1988)
6. L.A.M. Ruotolo, D.S. Santos-Junior and J.C. Gubulin, *Water Res.*, 40 (2006) 1555
7. G. Ondrey and A. Shanley, *Chem. Eng.*, 100 (1993) 47
8. M.E. Vallejo, P. Huguet, C. Innocent et al., *J. Phys. Chem. B*, 103 (1999) 11366
9. J. Khan, B.P. Tripathi, A. Saxena et al., *Electrochim. Acta*, 52 (2007) 6719
10. D. Zhao, A.K. SenGupta and L. Stewart, *Ind. Eng. Chem. Res.*, 37 (1998) 4383
11. S. Kocaoba and G. Akcin, *Desalination*, 180 (2005) 151
12. S. Rengaraj, K.H. Yeon and S.H. Moon, *J. Hazard. Mater.*, 87 (2001) 273
13. A.K. SenGupta, S. Subramanian and D. Clifford, *J. Environ. Eng.*, 114 (1988) 137
14. R. Molinari, E. Drioli and G. Pantano, *Sep. Sci. Technol.*, 24 (1989) 1015
15. E. Salazar, M.I. Ortiz, A.M. Urriaga et al., *Ind. Eng. Chem. Res.*, 31 (1992) 1516
16. Y. Kobuchi, H. Motomura, Y. Noma et al., *J. Membr. Sci.*, 27 (1986) 173
17. Y.S. Dzyazko, A. Mahmoud, F. Lapique, et al., *J. Appl. Electrochem.*, 37 (2007) 209
18. E. Castillo, M. Granados and J.L. Cortina, *Anal. Chim. Acta*, 464 (2002) 15
19. M.E. Vallejo, F. Persin, C. Innocent et al., *Sep. Purif. Technol.*, 21 (2000) 61
20. J. Lambert, M. Rakib, G. Durand et al., *Desalination*, 191 (2006) 100
21. L. Lebrun, N. Follain and M. Metayer, *Electrochim. Acta*, 50 (2004) 985
22. R.F.D. Costa, M.A.S. Rodriguez and J.Z. Ferreira, *Sep. Sci. Technol.*, 33 (1998) 1135
23. H.K. Hansen, A.B. Ribeiro, E.P. Mateus et al., *Electrochim. Acta*, 52 (2007) 3406
24. G.O. Mallory and J.B. Hajdu, *Electroless plating. Fundamentals and Applications*, American electroplaters and surface finishers society, New York (1990)
25. S. Sachdeva and A. Kumar, *J. Membr. Sci.*, 307 (2008) 37
26. N.V. Mandich, C.C. Lee and J.R. Selman, *Plat. Surf. Finish.*, 84 (1997) 82
27. S.L. Gudatti, T.M. Holsen, C-C. Li et al., *J. Appl. Electrochem.*, 29 (1999) 1129
28. M. García-Gabaldón, V. Pérez-Herranz, E. Sánchez et al., *J. Membr. Sci.*, 280 (2006) 536
29. M. García-Gabaldón, V. Pérez-Herranz, E. Sánchez et al., *J. Membr. Sci.*, 323 (2008) 213
30. M. García-Gabaldón, V. Pérez-Herranz, J. Garcia-Anton et al., *Sep. Purif. Technol.*, 45 (2005) 183
31. M. García-Gabaldón, V. Pérez-Herranz, J. Garcia-Anton et al., *Sep. Purif. Technol.*, 51 (2006) 143
32. M.I. Ahmed, T.M. Holsen and J.R. Selman, *J. Appl. Electrochem.*, 31 (2001)
33. A.F. Clifford, *Inorganic Chemistry of Qualitative Analysis*, 2nd ed., Prentice-Hall, Englewood Cliffs, NJ (1961)
34. H. Karami, B. Kafi and S.N. Mortazavi, *Int. J. Electrochem. Sci.*, 4 (2009) 414

35. H. Karami and M. Alipour, *Int. J. Electrochem. Sci.*, 4 (2009) 1511
36. K.R. Newby, *Metal Finishing*, 105 (2007) 182
37. A.J. Chaudhary, B. Ganguli and S.M. Grimes, *Chemosphere*, 62 (2006) 841
38. S. Vasudevan, G. Sozhan, S. Mohan et al., *Ind. Eng. Chem., Res.*, 46 (2007) 2898
39. I.Zongo, J. Leclerc, H. A. Maïga et al., *Sep. Purif. Technol.*, 66 (2009) 159
40. J.C. Bazan and J.M. Bisang, *J. Appl. Electrochem.*, 34 (2004) 501